Bioorganic Chemistry 91 (2019) 103071

Contents lists available at ScienceDirect

Bioorganic Chemistry

journal homepage: www.elsevier.com/locate/bioorg

Structural modifications and *in vitro* pharmacological evaluation of 4-pyridyl-piperazine derivatives as an active and selective histamine H_3 receptor ligands

Katarzyna Szczepańska[a], Tadeusz Karcz[a], Agata Siwek[b], Kamil J. Kuder[a], Gniewomir Latacz[a], Marek Bednarski[c], Małgorzata Szafarz[d], Stefanie Hagenow[e], Annamaria Lubelska[a], Agnieszka Olejarz-Maciej[a], Michał Sobolewski[a], Kamil Mika[c], Magdalena Kotańska[c], Holger Stark[e], Katarzyna Kieć-Kononowicz[a,*]

[a] Department of Technology and Biotechnology of Drugs, Faculty of Pharmacy, Jagiellonian University Medical College, Medyczna 9, Kraków 30-688, Poland
[b] Department of Pharmacobiology, Faculty of Pharmacy, Jagiellonian University Medical College, Medyczna 9, Kraków 30-688, Poland
[c] Department of Pharmacodynamics, Faculty of Pharmacy, Jagiellonian University Medical College, Medyczna 9, Kraków 30-688, Poland
[d] Department of Pharmacokinetics and Physical Pharmacy, Jagiellonian University Medical College, Medyczna 9, Kraków 30-688, Poland
[e] Institute of Pharmaceutical and Medicinal Chemistry, Heinrich Heine University Düsseldorf, Universitaetsstr. 1, 40225 Duesseldorf, Germany

ARTICLE INFO

Keywords:
Histamine H_3 receptor
Histamine H_3 receptor ligands
Non-imidazole histamine H_3R ligands
Piperazine derivatives
Selective ligands
Molecular docking
Metabolic stability

ABSTRACT

A novel series of 4-pyridylpiperazine derivatives with varying alkyl linker length and eastern part substituents proved to be potent histamine H_3 receptor (hH_3R) ligands in the nanomolar concentration range. While paying attention to their alkyl linker length, derivatives with a six methylene linker tend to be more potent than their five methylene homologues. Moreover, in the case of both phenoxyacetyl- and phenoxypropionyl- derivatives, an eight methylene linkers possess lower activity than their seven methylene homologues. However, in global analysis of collected data on the influence of alkyl linker length, a three methylene homologues appeared to be of highest hH_3R affinity among all described 4-pyridylpiperazine derivatives from our group up to date. In the case of biphenyl and benzophenone derivatives, compounds with *para*- substituted second aromatic ring were of higher affinity than their *meta* analogues. Interestingly, benzophenone derivative **18** showed the highest affinity among all tested compounds (hH_3R K_i = 3.12 nM). The likely protein-ligand interactions, responsible for their high affinity were demonstrated using molecular modeling techniques. Furthermore, selectivity, intrinsic activity at H_3R, as well as drug-like properties of selected ligands were evaluated using *in vitro* methods.

1. Introduction

Function of histamine as neurotransmitter has been proven with the discovery of the H_3 receptor [1,2]. It is presynaptically located as autoreceptor controlling the synthesis and release of histamine. As heteroreceptor it modulates with presynaptical localization the release of numerous other neurotransmitters, e.g. acetylcholine, norepinephrine, dopamine, serotonin, glutamate, γ-aminobutyric acid [3]. The histamine H_3 receptor is anatomically localized primarily to the Central Nervous System (CNS) with prominent expression in basal ganglia, hippocampus, cortex and striatal area [4]. In the periphery H_3R can be found with low density in gastrointestinal, bronchial and cardiovascular system. As H_3 autoreceptor activation stimulates the negative feed-back mechanism, reduced central histaminergic activity is observed. Involvement in cognition, sleep-wake status, energy homeostatic regulation, inflammation etc. has attracted pharmaceutical research for numerous so far unmet therapeutic approaches in different peripheral, but mainly central diseases [5,6]. The wide spectrum of possible therapeutic implications makes H_3Rs one of the most researched areas in the vast field of GPCR ligands – starting from imidazole containing ligands, through various non-imidazole derivatives, with recent introduction of successful *Wakix®* to pharmaceutical market.

One such replacement for an imidazole is a piperazine moiety, an important versatile scaffold in rational drug design for most of the GPCR ligands. It is one of the most inherent structural elements in drug finding, marked with a large variety of successes in biological applications. Appropriate physicochemical properties of the piperazine

* Corresponding author.
E-mail address: mfkonono@cyf-kr.edu.pl (K. Kieć-Kononowicz).

https://doi.org/10.1016/j.bioorg.2019.103071
Received 13 May 2019; Received in revised form 12 June 2019; Accepted 14 June 2019
Available online 20 June 2019

template make this molecular subunit a useful and well-positioned system in the search for new drugs. Furthermore, it acts as efficient and particular subject for a range of miscellaneous scientific objectives in medicinal chemistry and thus, piperazine moiety is regarded as privileged framework [7]. This scaffold is mainly observed in molecules targeting various CNS receptors, such as different subtypes of adrenergic, dopaminergic and serotoninergic receptors [8–10]. Therefore, paying attention to its versatile properties and pointing out that piperazine is also observed as a key structural feature in many histamine H_3R ligands (as a successful imidazole replacement), we focused on such derivatives in this work.

In general, all compounds presented herein fit the traditional pharmacophore model for histamine H_3R blocking compounds, that contain a basic moiety linked by a spacer to a central, mostly aromatic core structure which then is connected to further affinity enhancing elements, e.g. another basic moiety or hydrophilic/lipophilic groups or a combination thereof [11].

Structure-activity studies of previously described ligands allowed for the establishment of the 4-pyridyl-piperazine moiety a new bioisosteric piperidine replacement in H_3R ligands [12]. The results of the *in vitro* tests proved this scaffold as a crucial element for high hH3R affinity. Furthermore, modeling studies showed its role in the formation of suitable interactions with the hH_3R.

Therefore, we selected eight previously described compounds KSK29, KSK19, KSK30, KSK25, KSK3, KSK31, KSK9 and KSK32, presented in the Fig. 1, that served as lead structures for further modifications [12,13]. Considered compounds represent promising, very high H_3R antagonist potency, as well as interesting anticonvulsant, precognitive and anorectic pharmacological profile in several rodent models.

Structural modifications of leads performed within this work were divided into two phases. Phase 1 included:

- extension of the alkyl chain to 5–6 methylene groups,
- as well as (in the case of acetyl and propionyl derivatives generally more active than *tert*-butyl and *tert*-pentyl analogues) both: extension of linker up to 8 and subtraction to 2 methylene groups.

After the selection of optimal linker length (based on *in vitro* studies), in phase 2, various moieties (methyl, ethyl, phenyl, benzoyl) were introduced to the aromatic ring in eastern part of compounds.

Paying attention to structural similarity of concerned compounds to other GPCR ligands, determination of affinity to histamine H_1, dopamine D_2, muscarinic M_1 and α_1 adrenergic receptors was also carried out.

2. Results and discussion

2.1. Chemistry

The synthesis of desired final compounds **2–21** was achieved through the synthetic route presented in Scheme 1. According to the

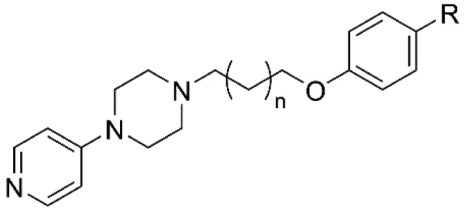

R = *tert*-butyl, n = 1 **KSK29** hH_3R K_i = 16.0 nM
R = *tert*-butyl, n = 2 **KSK19** hH_3R K_i = 37.8 nM

R = *tert*-pentyl, n = 1 **KSK30** hH_3R K_i = 30.6 nM
R = *tert*-pentyl, n = 2 **KSK25** hH_3R K_i = 120.0 nM

R = acetyl, n = 1 **KSK3** hH_3R K_i = 10.2 nM
R = acetyl, n = 2 **KSK31** hH_3R K_i = 115 nM

R = propionyl, n = 1 **KSK9** hH_3R K_i = 5.2 nM
R = propionyl, n = 2 **KSK32** hH_3R K_i = 15.4 nM

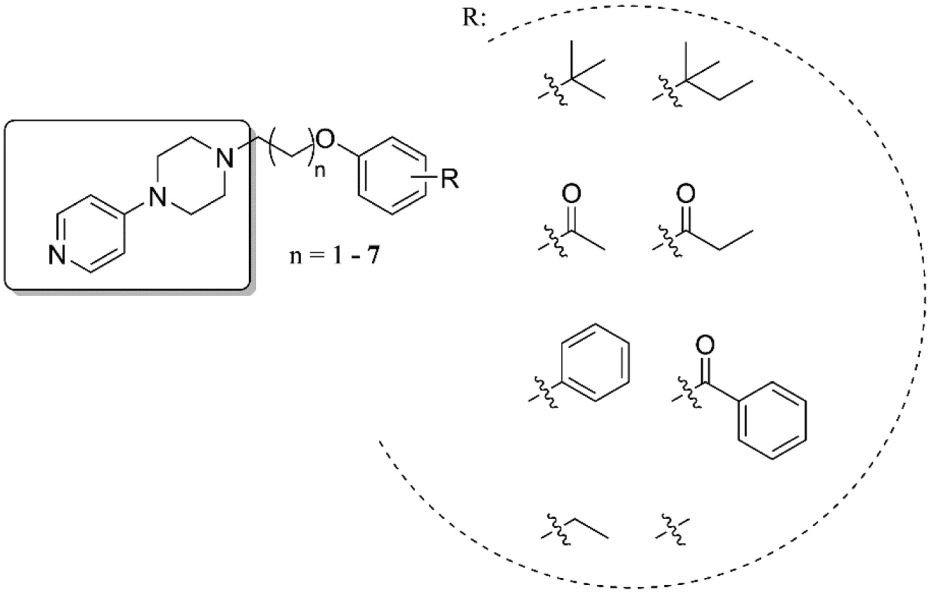

Fig. 1. KSK29, KSK19, KSK30, KSK25, KSK3, KSK31, KSK9, KSK32 and general structures of described ligands; hH_3R – human histamine H_3 receptor.

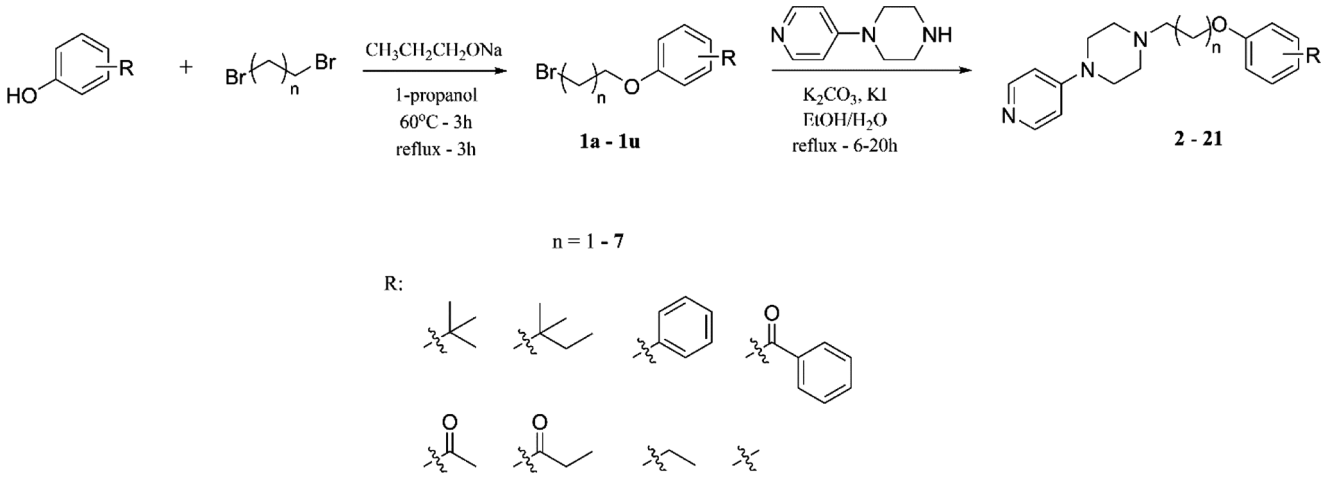

Scheme 1. General synthetic pathway for compounds **2–21**.

procedure [14] modified by us [12,13], the phenoxy alkyl bromides **1a–u** were obtained by one-step alkylation of commercially available phenols with α,ω-dibromoalkanes in propan-1-ol under reflux conditions. Obtained precursor bromides were then coupled with 1-(pyridin-4-yl)piperazine in the mixture of ethanol/water with powdered potassium carbonate and a catalytic amount of potassium iodide. Final products were obtained as free bases and isolated as oxalic acid salts.

2.2. Pharmacology

2.2.1. Histamine H_3 receptor affinity

All compounds (as oxalate salts) were tested in H_3R *in vitro* binding studies, using slightly modified methods to those described previously [15]. Briefly, compounds were tested at five to eleven appropriate concentrations in a [^{3}H]N^α–Methylhistamine (K_D = 3.08 nM) radioligand depletion assay to determine the affinity at human recombinant histamine H_3R stably expressed in HEK-293 cells.

In vitro affinity data are assembled in Table 1. Paying attention to the alkyl linker length, derivatives with either a five or a six methylene linker show similar affinity with a K_i value below 100 nM with the exception of compound **7** and **10** (hH_3R K_i = 115 and 397 nM, respectively). According to our assumptions, acetyl and propionyl derivatives tend to show a higher affinity at H_3R than *tert*-butyl and *tert*-pentyl analogues (**6**, **10**, **7**, **11** *vs*. **4**, **8**, **5** and **9**).

Table 1
Structures of compounds **2–21** and their *in vitro* histamine H_3 receptor (hH_3R) affinities. Given data represent mean values within the 95% confidence interval (CI).

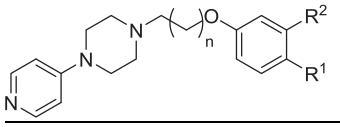

No.	N	R^1	R^2	hH_3R K_i [nM] x̄ [CI 95%]	No.	n	R^1	R^2	hH_3R K_i [nM] x̄ [CI 95%]
2	1		H	1957 [1212, 3158]	**12**	6		H	20.0 [13.6, 29.4]
3	1		H	1007 [622, 1630]	**13**	6		H	19.3 [6.57, 56.4]
4	4		H	29.9 [1.26, 708]	**14**	7		H	40.5 12.3, 134]
5	4		H	26.7 [15.9, 44.7]	**15**	7		H	38.9 [9.52, 159]
6	4		H	62.1 [7.02, 549]	**16**	2		H	21.1 [3.83, 116]
7	4		H	115 [26.8, 493]	**17**	2	H		53.6 [16.6, 174]
8	5		H	12.7 [4.35, 36.9]	**18**	2	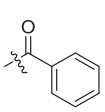	H	3.12 [0.66, 14.6]
9	5		H	16.9 [7.95, 36.0]	**19**	2	H	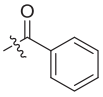	22.2 [3.30, 149]
10	5		H	397 [220, 715]	**20**	2	CH_2CH_3	H	40.4 [17.1, 95.9]
11	5		H	69.2 [29.6, 162]	**21**	2	CH_3	H	42.7 [12.4, 147]

Table 2
Radioligand binding assay for selected GPCRs. In the case of H_1, M_1 and D_2 receptors results are presented as a percentage of control specific binding at 1 and 0.1 μM concentration. Affinity to α_1 receptors are presented as K_i values.

Receptor	H_1		M_1		D_2		α_1
No.	% of control specific binding at 1 μM conc.	% of control specific binding at 0.1 μM conc.	% of control specific binding at 1 μM conc.	% of control specific binding at 0.1 μM conc	% of control specific binding at 1 μM conc.	% of control specific binding at 0.1 μM conc	K_i [nM] ± SEM
2	0	0	8	7	0	0	No affinity
3	0	0	4	1	0	0	No affinity
4	26	0	12	9	0	0	–
5	48	2	24	14	6	2	–
6	8	0	12	10	0	0	–
7	23	0	15	9	10	4	–
8	0	0	4	0	0	1	–
9	3	0	12	0	4	0	–
10	6	1	6	0	8	2	No affinity
11	30	6	11	0	14	4	No affinity
12	1	0	2	3	0	0	> 1000
13	10	0	18	11	0	0	> 5000
14	19	0	6	0	1	0	No affinity
15	14	0	16	0	0	1	No affinity
16	18	0	1	0	0	0	No affinity
17	15	2	15	8	15	10	> 5000
18	15	2	8	0	0	0	> 5000
19	7	0	11	4	10	0	> 5000
20	5	0	0	0	0	0	> 5000
21	11	0	0	3	0	0	3270.0 ± 320.0
KSK29	14	9	22	8	0	0	–
KSK19	3	0	2	0	3	0	> 5000
KSK30	15	8	28	12	0	3	–
KSK25	6	1	5	0	14	0	No affinity
KSK3	0	0	0	0	27	2	No affinity
KSK31	0	0	0	0	0	0	–
KSK9	0	0	3	0	0	0	No affinity
KSK32	0	1	0	0	3	1	–
Mepyramine	99	97	–	–	–	–	–
Triprolidine	100	99	–	–	–	–	–
Atropine	–	–	99	92	–	–	–
Scopolamine	–	–	100	98	–	–	–
Pirenzepine			89	45	–	–	–
Methoctramine	–	–	36	7	–	–	–
Haloperidol	–	–	–	–	98	93	–
Phentolamine	–	–	–	–	–	–	22.0 ± 1.5

In general, both phenoxyacetyl and -propionyl derivatives show high hH_3R affinity in low nanomolar concentration ranges with minor influences on affinity by extension of alkyl linker (**4**, **5**, **8**, **9**, **12–15**). However, a short ethylene linker results in reduction of affinity (**2** and **3**, hH_3R K_i = 1957 and 1007 nM, respectively).

Global analysis of collected data referring to influence of alkyl linker length, allowed for the selection of three methylene homologues as phase 2 templates, due to their highest H_3R affinity values among all described 4-pyridylpiperazine derivatives (see Fig. 1).

In order to determine the influence of substituents located in the "eastern part" of the molecule, various moieties were introduced to the aromatic ring of ligands. In the case of biphenyl and benzophenone derivatives, compounds with *para* position of the second aromatic ring tend to be of higher affinity than their *meta* analogues (**16** and **18** *vs*. **17** and **19**, hH_3R K_i = 21.1 and 3.12 nM *vs*. 53.6 and 22.2 nM). Interestingly, **18** showed the highest affinity among all tested 4-pyridylpiperazine compounds from our group up to date (see Fig. 1). High affinities of **20** and **21** (hH_3R K_i = 40.4 and 42.7 nM, respectively), might also indicate the tolerance of smaller alkyl substituents attached to the aromatic ring able to interact with the H_3R binding site.

Table 3
The IC_{50} values of tested compounds in antagonist dose-response assay, with reference agonist (R-α-Methylhistamine) used at a final concentration equivalent to its EC_{80} value.

No.	IC_{50} [nM] ± SEM
1	No fit curve
2	No fit curve
10	3.5 ± 0.5
11	No fit curve
12	299.7 ± 39.4
13	2600 ± 0.3
14	2430 ± 0.3
15	No fit curve
16	No fit curve
17	No fit curve
18	54.5 ± 4.1
19	386.1 ± 25.9
20	152.8 ± 20.1
21	78.8 ± 6.3
Clobenpropit	**3.4 ± 0.2**

2.2.2. Affinity to other GPCRs

In order to confirm selectivity of obtained ligands, determination of affinity to histamine H_1, dopamine D_2, muscarinic M_1 and α_1 adrenergic receptors was carried out (Table 2). In the case of H_1, D_2 and M_1R, radioligand binding was performed using membranes from CHO-K1 cells stably transfected with proper receptors. Adrenergic (α_1) receptor binding assay was performed using rat cortex tissue. All assays were carried out in duplicates. They clearly indicate high selectivity of herein and previously described 4-pyridylpiperazine derivatives for human H_3R.

Table 4
PAMPA results (permeability coefficient *Pe*) for selected compounds. CFN – well permeable standard Caffeine, NFX – low permeable standard Norfloxacin. ND*: No data, compound precipitated under assay conditions.

No.	*Pe* (10^{-6} cm/s) ± SD
11	ND*
12	7.29 ± 1.6
13	7.11 ± 3.3
14	6.22 ± 2.3
15	6.55 ± 0.8
16	7.36 ± 1.7
18	4.16 ± 0.7
CFN	**15.1 ± 0.4**
NFX	**0.56 ± 0.1**

2.2.3. Intrinsic activity at histamine H_3 receptor

In order to identify compounds that are antagonists, inverse agonists and/or partial agonists, efficacy of selected structures was assessed by luminescence detection of calcium mobilization in response to H_3R stimulation. None of the tested compounds showed agonistic activity towards the desired biological target (data not shown).

Of all compounds, only **10** showed comparable antagonist activity to the reference compound Clobenpropit (Table 3). The IC_{50} value for the antagonistic intrinsic activity of compound **10** is approximately 100 fold greater than the IC_{50} value for affinity at H_3R. The test used to determine the antagonistic activity is based on the evaluation of calcium mobilization in the cell. Therefore, this result may indicate an additional mechanism of compound **10**, which affects the mobilization of intracellular calcium. Explanation of this effect is subjected to our further studies. Compounds **18**, **20** and **21** showed antagonist activity, but with effective concentrations 16–37 times lower than the reference compound. Lowest antagonist potencies were demonstrated by **12**, **13**, **14** and **19** with the IC_{50} values in the range between 250 and 2600 nM. For the remaining tested compounds, it was not possible to fit a dose-response curve in that type of assay.

2.3. Results of selected ADMET parameters

2.3.1. Permeability profile

The ability of selected H_3R ligands to penetrate across lipid membranes was estimated by parallel artificial membrane permeability assay (PAMPA). In medicinal chemistry, PAMPA is a method which determines the passive diffusion of substances from a donor into acceptor compartment, through a lipid – infused artificial membrane. Passive diffusion it is the predominant mechanism for absorption of most commercial drugs [16]. The results were expressed as permeability coefficient *Pe* calculated according to the formulas provided by manufacturer [17]. The *Pe* values of tested compounds varies between 4.16 and 7.36 × 10^{-6} cm (Table 4). Considering gathered data and comparing it to two standards: well-permeable Caffeine (*Pe* = 15.1 × 10^{-6} cm/s) and low-permeable Norfloxacin (*Pe* = 0.56 × 10^{-6} cm/s), it seems reasonable to acknowledge studied molecules as substances with efficient passive transport through biological membranes.

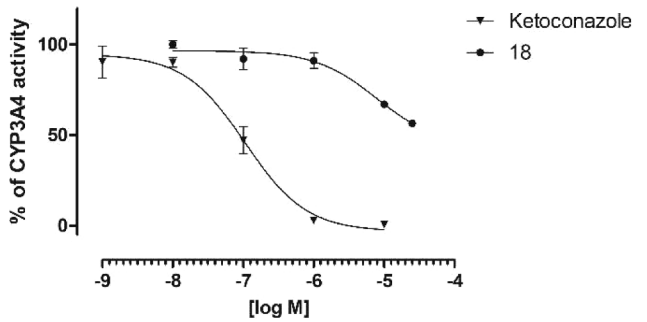

Fig. 2. The effect of **18** and the reference ketoconazole on CYP_{3A4} activity.

2.3.2. Influence on cytochrome P450 3A4 activity

In order to assess the potential risk of drug-drug interactions of most active ligand, the luminescence-based CYP3A4 P450-Glo™ assay was used. Compound **18** was incubated with recombinant CYP3A4 isoform for 30 min. The measurement of CYP3A4 activity showed slight inhibition of enzyme activity by **18**, but only at high micromolar concentrations (10 and 25 μM) (Fig. 2).

2.3.3. Hepatotoxicity – the effect on HepG2 cells

To predict potential hepatotoxicity of **16** and **18**, their antiproliferative activity at hepatoma HepG2 cells was evaluated. Statistically significant decrease in the cell viability was observed at 10 and 100 μM concentrations. However, this effect was weak, compared to reference compounds: doxorubicin (DX) and carbonyl cyanide 3-chlorophenylhydrazone (CCCP), which decreased viability of HepG2 by > 50% at 1 μM and 10 μM, respectively (Fig. 3).

2.3.4. Metabolic stability

Initially, computational tool MetaSite was used to determine the potential sites of metabolism of compound **18** [18]. The obtained data suggested the pyridine moiety as the most probable site of metabolism. Moreover, the aliphatic linker was also shown to be susceptible for metabolic biotransformation (see Supplementary Data).

Next, the metabolic stability was evaluated *in vitro* using mouse liver microsomes (MLMs). The LC/MS analysis of the reaction mixture after 120 min incubation of **18** with MLMs led to the identification of two metabolites with the following molecular masses of their quasimolecular ions $[M + H]^+$: m/z = 404.27 (**M1**, main metabolite) and m/z = 418.29 (**M2**, Fig. 4). In MS analysis, the observed molecular masses and ion fragments of **18**, as well as its main metabolite **M1** (+2 units) and **M2** (+16 units) suggest the ketone reduction and the reaction of hydroxylation as metabolic routes of compound **18**. However, according to the *in silico* data, either *N*-oxidation or hydroxylation were proposed, which occurred most probably at the 4-pyridyl moiety (see Supplementary Data). In summary, **18** showed moderate metabolic stability, as ~42% remained in the reaction mixture, with ketone reduction as the main metabolic pathway (Fig. 4).

2.4. Molecular modeling

Although the number of GPCRs crystal structure is continuously growing, structure of only one member of histamine receptor family was resolved up to date: histamine H_1 receptor (PDB ID: 3RZE [19]). Therefore, in this study previously built and described H_3R homology model (with reference ligand Pitolisant in the binding pocket) was used [12].

All of the docking poses presented binding mode perpendicular to membrane plane, in agreement with findings of Levoin et al. [20], with *p*-propionyl and *p*-acetyl derivatives scored with highest and lowest scores respectively. For most of the compounds, necessary hH_3R antagonist/inverse agonist interactions were found: hydrogen bond and/or salt bridge formation between protonated piperazine nitrogen and $GLU206^{5.46}$ (upper case numeration according to Balesteros-Weinstein [21]). Moreover, formation of H-bond between $TYR374^{6.51}$ and the ether oxygen for compounds with alkyl chain up to five methylene groups (e.g. **4** and **16**) was observed.

Similarly to our previous findings, π-π stabilization of a 4-pyridyl moiety by either indole or benzene ring of $TRP371^{6.48}$ was observed. Since this residue appears as one of the so-called molecular switches of the GPCR's [22], herefound interactions might influence high affinity of the described ligands. In turn, benzene rings of the lipophilic part of ligands were also stabilized through π-π stacking with at least one of

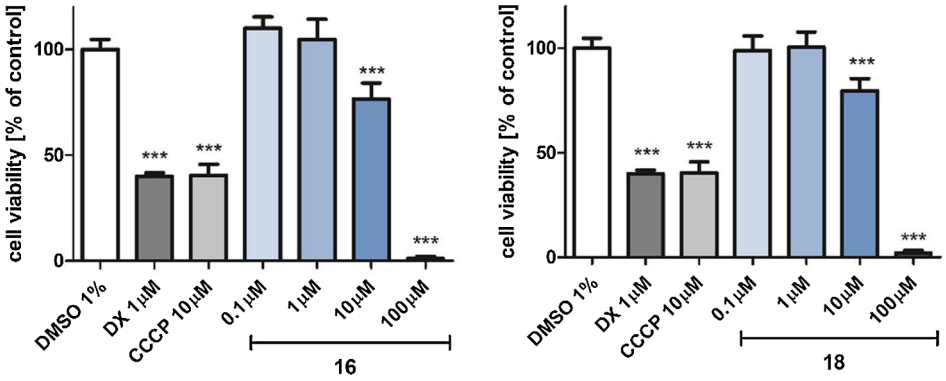

Fig. 3. HepG2 cell viability after 72 h–long incubation with compounds **16**, **18**, Doxorubicin (DX) and CCCP. The statistical significance was evaluated by a one-way ANOVA, followed by Bonferroni's Comparison Test ($^{***}p < 0.001$ compared with negative control).

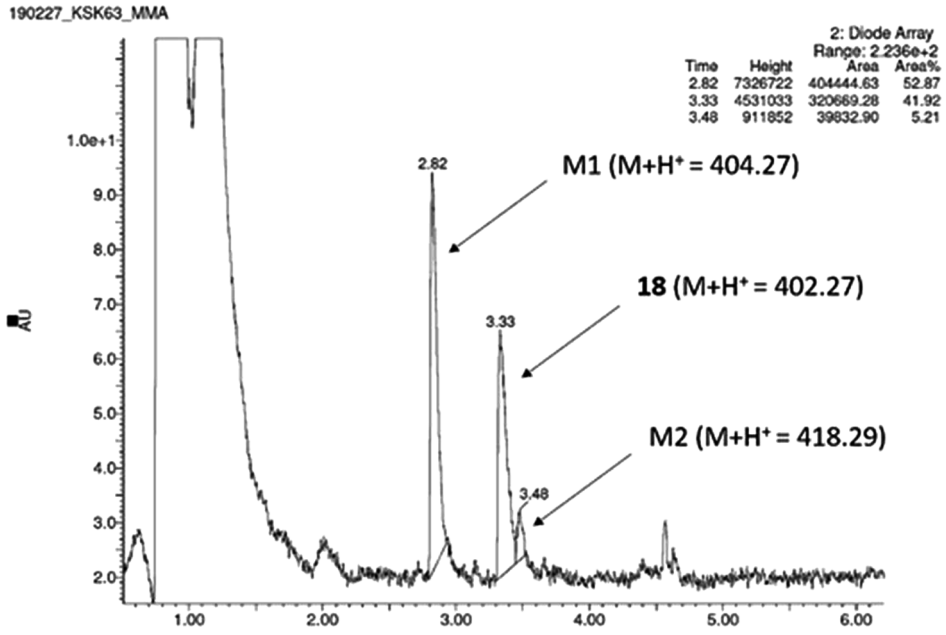

Fig. 4. The UPLC spectrum of reaction mixture after 2 h incubation of **18** with MLMs.

aminoacids: TYR115$^{3.33}$, TYR394$^{7.35}$, TYR189$^{45.51}$, PHE193 (ECL2). For most of the compounds, formation of hydrogen bond(s) between carbonyl group oxygen and ARG381$^{6.58}$ amine groups was found. On the other hand, in the case of biphenyl compound **16**, terminal benzene ring formed a π-cation interaction with ARG381$^{6.58}$ (Fig. 5), along with previously mentioned π-π stacking stabilization, which was not found for the slightly less affine *meta* substituted derivative **17**. Similar findings were found for benzophenone derivatives **18** and **19**, where meta derivative was derived of π-π stacking stabilization of terminal benzene ring, when compared to its *para* analogue, thus yielding in slightly lower affinity (Fig. 6).

In some cases for compounds of 6–8 methylene groups alkyl chain, a slightly rotated along Y-axis poses were obtained, resulting in H-bond formation between TYR91$^{2.61}$ (instead of ARG381$^{6.58}$) hydroxyl moiety and carbonyl group oxygen. However, paying attention to overall high H_3R affinity in tested group and overall observed ligand-receptor interactions such poses and interactions might have no pharmacological coverage.

3. Conclusions

The investigated series of novel 4-pyridylpiperazine derivatives proved to be potent histamine H_3R ligands (hH_3R K_i = 3.12 nM − 1.96 μM). Focusing on the alkyl linker length (five to eight methylene linker), independently of bulky, eastern part substituents, derivatives show similar H_3R affinity with exception of **7** and **10**. However, a short ethylene linker led to reduction of the hH_3R affinity. Overall, three methylene homologues showed the highest affinity values among all described 4-pyridylpiperazine derivatives.

In order to determine the influence of substituents located in the "eastern part" of the molecule, various moieties were introduced to the aromatic ring of ligands resulting in only slight variations regarding H_3R affinity. Acetyl and propionyl as well as *tert*-butyl and *tert*-pentyl showed generally high affinity H_3R with few exceptions. Even larger substituents, namely biphenyl and benzophenone derivatives, were tolerated by the H_3R. Interestingly, benzophenone derivative **18** showed the highest affinity among all tested compounds so far (hH_3R K_i = 3.12 nM). Docking studies to histamine H_3R homology model allowed the observation of previously proposed ligand-receptor interactions. Selectivity of obtained compounds was confirmed in radioligand binding assays with histamine H_1, dopamine D_2, muscarinic M_1 and α_1 adrenergic receptors. In order to determine functional activity of the compounds, efficacy of selected structures was assessed by luminescence detection of calcium mobilization in response to H_3R stimulation. In fact, of all compounds, **10**, **18**, **20** and **21** showed antagonist activity with nanomolar effective concentrations. Finally, a series of novel 4-

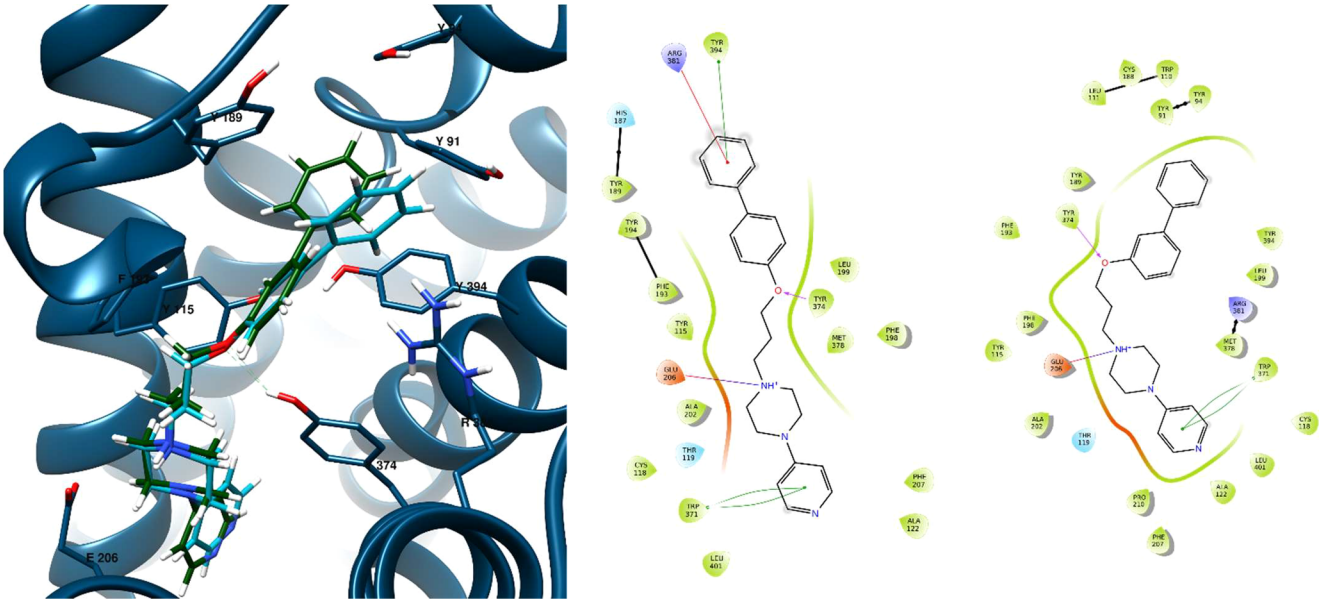

Fig. 5. Left panel: calculated binding pose for ligands **16** (light blue) and **17** (dark green) in histamine H_3 homology receptor binding pocket; middle panel & right panel: ligand interaction diagrams for compounds **16** and **17** respectively.

pyridylpiperazine derivatives proved to be active and selective histamine H_3R blocking compounds. Determination of their pharmacological profile is subjected to our further research.

4. Experimental protocols

4.1. Chemistry

4.1.1. General synthetic procedure for compounds **1a–1u**

All compounds were obtained using methods described previously [12,13]. Detailed synthetic procedure could be found in Supplementary Data.

4.1.2. General synthetic procedure for compounds **2–21**

All compounds were obtained using methods described previously [12,13]. Detailed synthetic procedure and analytical data could be found in Supplementary Data.

4.2. Pharmacology

4.2.1. $[^3H]N^{\alpha}$-Methylhistamine hH_3R displacement assay

Competition binding data were analyzed using GraphPad Prism (V6.01, San Diego, CA, USA) software, using non-linear least squares/ regression fit. K_i values were calculated from IC_{50} values according to Cheng-Prusoff equation [23]. Statistic analysis was performed on pK_i values from at least three experiments, each performed at least in

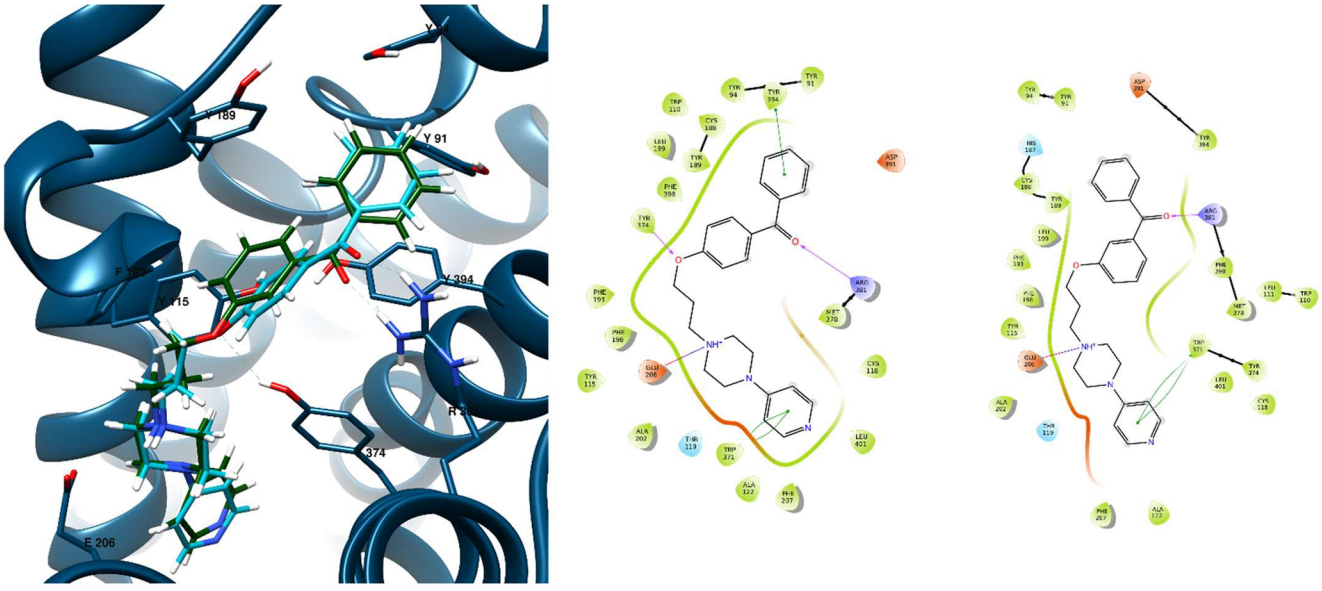

Fig. 6. Left panel: calculated binding pose for ligands **18** (light blue) and **19** (dark green) in histamine H_3 homology receptor binding pocket; middle panel & right panel: ligand interaction diagrams for compounds **18** and **19** respectively.

duplicates. Mean affinity values (K_i) were transferred into nanomolar concentrations (with 95% confidence interval). The displacement binding assay was carried out as described by Kottke et al. with slight modifications [12,13,15].

4.2.2. Affinity at other GPCRs

4.2.2.1. Affinity at H_1 receptors. 10 mM stock solutions of tested compounds were prepared in DMSO. Serial dilutions of compounds were prepared in 96-well microplate in assay buffers using automated pipetting system epMotion 5070 (Eppendorf). Each compound was tested in a screening assay at the final concentrations of 1 μM and 0.1 μM. Results were expressed as percent inhibition of [^{3}H]-Pyrilamine binding. Reference compounds were tested in eight concentrations from 10^{-5} to 10^{-12} M (final concentration). Radioligand binding was performed using membranes from CHO-K1 cells stably transfected with the human histaminergic H_1 receptor. All assays were carried out in duplicates. 50 μl working solution of the tested compounds, 50 μl [^{3}H]-Pyrilamine (spec. act. 20.0 Ci/mmol, final concentration 1.5 nM) and 150 μl diluted membranes (5 μg protein per well) prepared in assay buffer (50 mM Tris-HCl, pH 7.4; 5 mM $MgCl_2$) were transferred to polypropylene 96-well microplate using 96-wells pipetting station Rainin Liquidator (MettlerToledo). Mepyramine (10 μM) was used to define nonspecific binding. Microplate was covered with a sealing tape, mixed and incubated for 60 min at 27 °C. The reaction was terminated by rapid filtration through GF/B filter mate presoaked with 0.5% polyethyleneimine for 30 min. Five rapid washes with 300 μl 50 mM Tris buffer (4 °C, pH 7.4) were performed using 96-well FilterMate harvester (PerkinElmer, USA). The filter mates were dried at 37 °C in forced air fan incubator and then solid scintillator MeltiLex was melted on filter mates at 90 °C for 4 min. Radioactivity was counted in MicroBeta2 scintillation counter (PerkinElmer). Data were fitted to a one-site curve-fitting equation with Prism 5 (GraphPad Software) and K_i values were estimated from the Cheng–Prusoff equation.

4.2.2.2. Affinity at M_1 receptors. 10 mM stock solutions of tested compounds were prepared in DMSO. Serial dilutions of compounds were prepared in 96-well microplate in assay buffers using automated pipetting system epMotion 5070 (Eppendorf). Each compound was tested in a screening assay at the final concentrations of 1 μM and 0.1 μM. Results were expressed as percent inhibition of [^{3}H]-N^{α}-Scopolamine binding. Reference compounds were tested in 8 concentrations from 10^{-5} to 10^{-12} M (final concentration). Radioligand binding was performed using membranes from CHO-K1 cells stably transfected with the human M_1 receptor. All assays were carried out in duplicates. 50 μl working solution of the tested compounds, 50 μl [^{3}H]-Scopolamine (spec. act. 84.1 Ci/mmol, final concentration 0.2 nM) and 150 μl diluted membranes (35 μg protein per well) prepared in assay buffer (PBS, pH 7.4) were transferred to polypropylene 96-well microplate using 96-wells pipetting station Rainin Liquidator (MettlerToledo). Atropine (10 μM) was used to define nonspecific binding. Microplate was covered with a sealing tape, mixed and incubated for 120 min at 27 °C. The reaction was terminated by rapid filtration through GF/A filter mate presoaked with 0.5% polyethyleneimine for 30 min. Five rapid washes with 300 μl 50 mM Tris buffer (4 °C, pH 7.4) were performed using 96-well FilterMate harvester (PerkinElmer, USA). The filter mates were dried at 37 °C in forced air fan incubator and then solid scintillator MeltiLex was melted on filter mates at 90 °C for 4 min. Radioactivity was counted in MicroBeta2 scintillation counter (PerkinElmer). Data were fitted to a one-site curve-fitting equation with Prism 5 (GraphPad Software) and K_i values were estimated from the Cheng–Prusoff equation.

4.2.2.3. Affinity at D_2 receptors. 10 mM stock solutions of tested compounds were prepared in DMSO. Serial dilutions of compounds were prepared in 96-well microplate in assay buffers using automated pipetting system epMotion 5070 (Eppendorf). Each compound was tested in a screening assay at the final concentrations of 1 μM and 0.1 μM. Results were expressed as percent inhibition of [^{3}H]-Methylspiperone binding. Radioligand binding was performed using membranes from CHO-K1 cells stably transfected with the human D_2 receptor (PerkinElmer). All assays were carried out in duplicates. 50 μl working solution of the tested compounds, 50 μl [^{3}H]-Methylspiperone (final concentration 0.4 nM) and 150 μl diluted membranes (3 μg protein per well) prepared in assay buffer (50 mM Tris, pH 7.4, 50 mM HEPES, 50 mM NaCl, 5 mM $MgCl_2$, 0.5 mM EDTA) were transferred to polypropylene 96-well microplate using 96-wells pipetting station Rainin Liquidator (MettlerToledo). Haloperidol (10 μM) was used to define nonspecific binding. Microplate was covered with a sealing tape, mixed and incubated for 60 min at 37 °C. The reaction was terminated by rapid filtration through GF/B filter mate presoaked with 0.5% polyethyleneimine for 30 min. Ten rapid washes with 200 μl 50 mM Tris buffer (4 °C, pH 7.4) were performed using automated harvester system Harvester-96 MACH III FM (Tomtec). The filter mates were dried at 37 °C in forced air fan incubator and then solid scintillator MeltiLex was melted on filter mates at 90 °C for 5 min. Radioactivity was counted in MicroBeta2 scintillation counter (PerkinElmer).

4.2.2.4. Affinity at α_1 receptors. 10 mM stock solutions of tested compounds were prepared in DMSO. Serial dilutions of compounds were prepared in 96-well microplate in assay buffers using automated pipetting system epMotion 5070 (Eppendorf). Each compound was tested in 6 concentrations from 10^{-5} to 10^{-10} M (final concentration). Radioligand binding was performed using tissue rat cortex. All assays were carried out in duplicates. 50 μl working solution of the tested compounds, 50 μl [^{3}H]-Prazosin (final concentration 0.2 nM) and 150 μl tissue suspension prepared in assay buffer (50 mM Tris-HCl, pH 7.6) were transferred to polypropylene 96-well microplate using 96-wells pipetting station Rainin Liquidator (MettlerToledo). Phentolamine (10 μM) was used to define nonspecific binding. Microplate was covered with a sealing tape, mixed and incubated for 30 min at 30 °C. The reaction was terminated by rapid filtration through GF/B filter mate. Ten rapid washes with 200 μl 50 mM Tris buffer (4 °C, pH 7.6) were performed using 96-well FilterMate harvester (PerkinElmer, USA). The filter mates were dried at 37 °C in forced air fan incubator and then solid scintillator MeltiLex was melted on filter mates at 90 °C for 4 min. The radioactivity on the filter was measured in MicroBeta TriLux 1450 scintillation counter (PerkinElmer, USA). Data were fitted to a one-site curve-fitting equation with Prism 6 (GraphPad Software) and K_i values were estimated from the Cheng–Prusoff equation.

4.2.3. Intrinsic activity at histamine H_3 receptor

The intrinsic activity at H_3R was assessed by luminescence detection of calcium mobilization using the recombinant jellyfish photoprotein, aequorin. Measurements were performed with Histamine H_3 AequoScreen cell line (PekinElmer cat. no. ES-392-A). The cell density in 96-well format measurements was 5000 cells per well. Cell harvesting, coelenterazine h (Invitrogen, cat. no. C 6780) loading and preparation were done according to instructions presented in the AequoScreen Starter Kit Manual. Compounds stock solutions were diluted in assay buffer (D-MEM/F-12, Invitrogen cat. no. 11039) containing 0.1% BSA (Intergen, cat. no. 3440-75) and pipetted (50 μl/well) into white ½ Area Plate – 96 well microplates (PerkinElmer, cat. no. 6005560). In the next step cell suspension was dispensed into plate wells using the POLARstar optima reader injectors.

Detection of agonist activity. *R*-α-Methylhistamine dihydrochloride (Sigma, Cat. no. H128) was used as an agonist for histamine H_3 receptor. Compounds dilution series in four replicates were prepared as instructed in the AequoScreen Starter Kit Manual. Emitted light was recorded for 20 s.

Detection of antagonist activity. For the antagonist assay, cells were injected (50 μl) into the assay plate with antagonists (50 μl) using the

POLARstar optima reader. The antagonist dilution series in four replicates were prepared as instructed in the AequoScreen Starter Kit Manual in concentrations from 10^{-11} to 10^{-6} M. Antagonist used for the histamine H_3 cell line was Clobenpropit (Sigma, cat. no. C209). Agonist (*R*-α-Methylhistamine dihydrochloride) at a single concentration was injected (50 µl, final concentration EC_{80}) on the preincubated (15–20 min) mixture of cells + antagonist and the emitted light was recorded for 20 s.

4.3. Analysis of selected ADMET parameters

4.3.1. Reference compounds

The compounds used as the references: Caffeine (CFN), carbonyl cyanide 3-chlorophenylhydrazone (CCCP), Doxorubicin (DX), Ketoconazole (KE), Norfloxacin (NFX) were obtained from Sigma-Aldrich (St. Louis, MO, USA).

4.3.2. Cell line

Hepatoma HepG2 (ATCC® HB-8065™) cell line used in the hepatotoxicity study was kindly donated by the Department of Pharmacological Screening, Jagiellonian University Medical College. The cell culture growth conditions were as described before [13,24–26].

4.3.3. Permeability across lipid membranes

Pre-coated PAMPA Plate System Gentest™ was obtained from Corning, (Tewksbury, MA, USA). It consists of 96-well receiver filter plate that has been pre-coated with structured layers of phospholipids and a matched donor microplate. The stock solutions of H_3R antagonists and reference drugs were diluted in the PBS buffer (pH 7.4) to the final concentration 200 µM. The compounds were applied into the donor wells (200 µl) and incubated (5 h) at RT. By using the UPLC-MS spectrometry (Waters ACQUITY™ TQD system with the TQ Detector, Waters, Milford, USA) with an internal standard the exact quantity of molecules that penetrated from donor to acceptor wells through phospholipid membrane was estimated. The permeability coefficients (*Pe*, cm/s) were calculated using the formula provided by the PAMPA Plate System manufacturer [17].

4.3.4. Influence on CYP3A4 activity

Luminescent CYP3A4 P450-Glo™ kit was obtained from Promega® (Madison, WI, USA). The assay was performed according to the protocol provided by the manufacturer and as described before [24–26]. Test and reference compounds were analyzed in triplicates. The luminescent signal was measured using a microplate reader EnSpire PerkinElmer (Waltham, MA, USA).

4.3.5. Hepatotoxicity – the effect on HepG2 cells

The H_3R antagonists' influence on HepG2 cells was evaluated according to the procedures described before [13,24–26]. Cell viability was determined after 72 h incubation (37 °C, 5% CO_2) with tested compounds in serial dilutions (0.1–100 µM) by CellTiter 96® AQueous One Solution Cell Proliferation Assay (MTS) obtained from Promega® (Madison, WI, USA). The absorbance was recorded at 490 nm using a 96-well plate reader (EnSpire, Perkin Elmer). As positive controls, cells were treated with Doxorubicin (1 µM) and mitochondrial toxin CCCP (10 µM).

4.3.6. Metabolic stability

In silico investigation was performed by MetaSite 6.0.1 provided by Molecular Discovery Ltd. The most probable sites of metabolism were predicted during this study by liver computational model [18]. All experiments were performed as described before [12,13,24,25]. Mass spectra were recorded on LC/MS system consisted of a Waters Acquity UPLC, coupled to a Waters TQD mass spectrometer (electro spray ionization mode ESI-tandem quadrupole).

4.4. Molecular modeling

For docking purposes, Schrödinger Maestro Suite (v. 11.5.011, Release 2018–01) was used [27]. Ligands were built in their ionized forms (protonated N4 piperazine nitrogen, structure charge +1) using crystal structure of compound KKB-4 [28] as a template. Bioactive conformations were generated using ConfGen module [29,30] (Force field: OPLS3, water environment; minimization method: PRCG with max. iterations of 2500 and convergence threshold of 0.05; conformational search of 100 steps per rotational bond). For all of the compounds 5 lowest energy conformers were selected for docking studies. Binding site was centered on ligand placed in homology model (Pitolisant). Docking to rigid form of receptor was performed using Glide module [31–33] (precision standard, flexible ligand sampling, max. 5 poses per conformer). Ligands were rated according to their position in binding pocket, interactions with binding pocket amino acids, as well as the docking score value. Ligand interaction diagrams were generated using Schrödinger Maestro, ligand-receptor visualizations were generated using UCSF Chimera [34].

Acknowledgements

We are pleased to acknowledge the generous support of the grant DFG INST 208/664-1 FUGG (HS), COST Action CA15135 (KKK, HS) and National Science Center, Poland granted on the basis of decision Nos. 2016/23/N/NZ7/00469 and 2016/23/B/NZ7/01063.

Appendix A. Supplementary material

Supplementary data to this article can be found online at https://doi.org/10.1016/j.bioorg.2019.103071.

References

[1] J.M. Arrang, M. Garbarg, J.C. Schwartz, Auto-inhibition of brain histamine release mediated by a novel class (H3) of histamine receptor, Nature 28 (1983) 832–837.
[2] M. Walter, H. Stark, Histamine receptor subtypes: a century of rational drug design, Front. Bio. Sci. 4 (2012) 461–488.
[3] M. Berlin, C.W. Boyce, M. de Lera Ruiz, Histamine H3 receptor as a drug discovery target, J. Med. Chem. 54 (2011) 26–53.
[4] D. Łażewska, K. Kieć-Kononowicz, New developments around histamine H_3 receptor antagonists/inverse agonists: a patent review (2010 – present), Expert Opin. Ther. Pat. 24 (1) (2014) 89–111.
[5] E. Tiligada, K. Kyriakidis, P.L. Chazot, M.B. Passani, Histamine pharmacology and new CNS drug targets, CNS Neurosci. Ther. 17 (2011) 620–628.
[6] (a) M. Incerti, L. Flammini, F. Saccani, G. Morini, M. Comini, M. Coruzzi, E. Barocelli, V. Ballabeni, S. Bertoni, Dual-acting drugs: an in vitro study of non-imidazole histamine H3 receptor antagonists combining anticholinesterase activity, ChemMedChem 5 (2010) 1143–1149;
(b) S. Hagenow, O.M. Bautista-Aguilera, A. Palomino-Antolin, V. Farree-Alins, L. Ismaili, P.L. Joffrin, M.L. Jimeno, O. Soukup, J. Janockova, L. Kalinowsky, E. Proschak, I. Iriepa, I. Moraleda, J.S. Schwed, A.R. Martinez, F. Lopez-Munoz, M. Chioua, J. Egea, R.R. Ramsay, J. Marco-Contelles, H. Stark, Multitarget-directed ligands combining cholinesterase and monoamine oxidase inhibition with histamine H3R antagonism for neurodegenerative diseases, Angew. Chem. Int. Ed. 56 (2017) 12765–12769.
[7] K. Szczepańska, K.J. Kuder, K. Kieć-Kononowicz, Histamine H3 Receptor Ligands in the Group of (Homo)piperazine Derivatives, Curr. Med. Chem. 25 (2018) 1609–1626.
[8] A.K. Rathi, R. Syed, H.S. Shin, R.V. Patel, Piperazine derivatives for therapeutic use: a patent review (2010-present), Expert Opin. Ther. Pat. 26 (2016) 777–797.
[9] M. Rosini, M.L. Bolognesi, D. Giardina, A. Minarini, V. Tumiatti, C. Melchiorre, Recent advances in alpha1-adrenoreceptor antagonists as pharmacological tools and therapeutic agents, Curr. Top. Med. Chem. 7 (2007) 147–162.
[10] V. SosKic, J. Joksimovic, Bioisosteric approach in the design of new dopaminergic/serotonergic ligands, Curr. Med. Chem. 5 (1998) 493–512.
[11] D. Łażewska, K. Kieć-Kononowicz, New developments around histamine H3 receptor antagonists/inverse agonists: a patent review (2010 – present), Expert Opin. Ther. Pat. 24 (2014) 89–111.
[12] K. Szczepańska, T. Karcz, S. Mogilski, A. Siwek, K.J. Kuder, G. Latacz, M. Kubacka, S. Hagenow, A. Lubelska, A. Olejarz, M. Kotańska, B. Sadek, H. Stark, K. Kieć-Kononowicz, Synthesis and biological activity of novel *tert*-butyl and *tert*-pentyl-phenoxyalkyl piperazine derivatives as histamine H_3R ligands, Eur. J. Med. Chem. 152 (2018) 223–234.
[13] K. Szczepańska, T. Karcz, M. Kotańska, A. Siwek, K.J. Kuder, G. Latacz, S. Mogilski,

S. Hagenow, A. Lubelska, M. Sobolewski, H. Stark, K. Kieć-Kononowicz, Optimization and preclinical evaluation of novel histamine H_3 receptor ligands: acetyl and propionyl phenoxyalkyl piperazine derivatives, Bioorg. Med. Chem. 26 (2018) 6056–6066.

[14] A. Alter, Disubstituted piperazines useful as schistosomiasis, Agents (1966) US3270004.

[15] (a) T. Kottke, K. Sander, L. Weizel, E.H. Schneider, S. Seifert, H. Stark, Receptorspecific functional efficacies of alkyl imidazoles as dual histamine H3/H4 receptor ligands, Eur. J. Pharmacol. 654 (2011) 200–208;
(b) M.A. Khanfar, D. Reiner, S. Hagenow, H. Stark, Design, synthesis, and biological evaluation of novel oxadiazole- and thiazole-based histamine H3R ligands, Bioorg. Med. Chem. 26 (2018) 4034–4046.

[16] L. Di, E. Kerns, Drug-Like Properties – Concepts, Structure Design and Methods: From ADME to Toxicity Optimization, second ed., 2016.

[17] X.X. Chen, A. Murawski, K. Patel, C.L. Crespi, P.V. Balimane, A novel design of artificial membrane for improving the PAMPA model, Pharm. Res. 25 (2008) 1511–1520.

[18] G. Cruciani, E. Carosati, E. De Boeck, K. Ethirajulu, C. Mackie, T. Howe, R. Vianello, MetaSite: understanding metabolism in human cytochromes from the perspective of the chemist, J. Med. Chem. 48 (22) (2005) 6970–6979.

[19] T. Shimamura, M. Shiroishi, S. Weyand, H. Tsujimoto, G. Winter, V. Katritch, R. Abagyan, V. Cherezov, W. Liu, G.W. Han, T. Kobayashi, R.C. Stevens, Structure of the human histamine H_1 receptor complex with doxepin, Nature 475 (2011) 65–70.

[20] N. Levoin, O. Labeeuw, S. Krief, T. Camels, O. Poupardin-Olivier, I. Berrebi-Bertrand, J.-M. Lecomte, J.-C. Schwartz, M. Capet, Determination of the binding mode and interacting amino-acids for dibasic H_3 receptor antagonists, Bioorg. Med. Chem. 21 (2013) 4526–4529.

[21] J.A. Ballesteros, H. Weinstein, Integrated methods for the construction of three-dimensional models and computational probing of structure-function relations in G protein-coupled receptors, Meth. Neurosci. 25 (1995) 366–428.

[22] B. Trzaskowski, D. Latek, S. Yuan, U. Ghoshdastider, A. Debinski, S. Filipek, Action of molecular switches in GPCRs -theoretical and experimental studies, Curr. Med. Chem. 19 (2012) 1090–1109.

[23] Y. Cheng, W.H. Prusoff, Relationship between the inhibition constant (Ki) and the concentration of inhibitor which causes 50 per cent inhibition (I50) of an enzymatic reaction, Biochem. Pharmacol. 22 (1973) 3099–3108.

[24] G. Latacz, A. Lubelska, M. Jastrzębska-Więsek, A. Partyka, A. Sobiło, A. Olejarz, K. Kucwaj-Brysz, G. Satała, A.J. Bojarski, A. Wesołowska, K. Kieć-Kononowicz, J. Handzlik, In the search for a lead structure among series of potent and selective hydantoin 5-HT_7R agents: the drug-likeness *in vitro* study, Chem. Biol. Drug Des. 90 (2017) 1295–1306.

[25] G. Latacz, A. Lubelska, M. Jastrzębska-Więsek, A. Partyka, K. Kucwaj-Brysz, A. Wesołowska, K. Kieć-Kononowicz, J. Handzlik, MF-8, a novel promising arylpiperazine-hydantoin based 5-HT7receptor antagonist: *In vitro* drug-likeness studies and *in vivo* pharmacological evaluation, Bioorg. Med. Chem. Lett. 28 (5) (2018) 878–883.

[26] G. Latacz, A.S. Hogendorf, A. Hogendorf, A. Lubelska, J.M. Wierońska, M. Woźniak, P. Cieślik, K. Kieć-Kononowicz, J. Handzlik, A.J. Bojarski, Search for a 5-CT alternative. *In vitro* and *in vivo* evaluation of novel pharmacological tools: 3-(1-alkyl-1H-imidazol-5-yl)-1H-indole-5-carboxamides, low-basicity 5-HT_7 receptor agonists, MedChemComm 9 (2018) 1882–1890.

[27] Schrödinger Release 2018-1: Schrödinger Suite 2016-1 Protein Preparation Wizard; Epik, Schrödinger, LLC, New York, NY, 2018.

[28] K. Kucwaj-Brysz, R. Kurczab, E. Żesławska, A. Lubelska, M.A. Marć, G. Latacz, G. Satała, W. Nitek, K. Kieć-Kononowicz, J. Handzlik, The role of aryl-topology in balancing between selective and dual 5-HT_7R/5-HT_{1A} actions of 3,5-substituted hydantoins, Med. Chem. Commun. 9 (2018) 1033.

[29] Schrödinger Release 2018-1: ConfGen, Schrödinger, LLC, New York, NY, 2018.

[30] K.S. Watts, P. Dalal, R.B. Murphy, W. Sherman, R.A. Friesner, J.C. Shelley, ConfGen: a conformational search method for efficient generation of bioactive conformers, J. Chem. Inf. Model. 50 (2010) 534–546.

[31] Schrödinger Release 2018-1: Glide, Schrödinger, LLC, New York, NY, 2018.

[32] T.A. Halgren, R.B. Murphy, R.A. Friesner, H.S. Beard, L.L. Frye, W.T. Pollard, J.L. Banks, Glide: a new approach for rapid, accurate docking and scoring. 2. Enrichment factors in database screening, J. Med. Chem. 47 (2004) 1750–1759.

[33] R.A. Friesner, R.B. Murphy, M.P. Repasky, L.L. Frye, J.R. Greenwood, T.A. Halgren, P.C. Sanschagrin, D.T. Mainz, Extra precision glide: docking and scoring incorporating a model of hydrophobic enclosure for protein−ligand complexes, J. Med. Chem. 49 (2006) 6177–6196.

[34] E.F. Pettersen, T.D. Goddard, C.C. Huang, G.S. Couch, D.M. Greenblatt, E.C. Meng, T.E. Ferrin, U.C.S.F. Chimera, A visualization system for exploratory research and analysis, J. Comput. Chem. 25 (2004) 1605–1612.